Renewable Energy 83 (2015) 171–187

Contents lists available at ScienceDirect

Renewable Energy

journal homepage: www.elsevier.com/locate/renene

Finding gaps on power production assessment on WECs: Wave definition analysis

A.D. de Andrés [a], R. Guanche [a, *], J. Weber [a, b], R. Costello [a, b]

[a] Environmental Hydraulics Institute – IH Cantabria, University of Cantabria, Isabel Torres 15, PCTCAN, Santander, Spain
[b] Centre for Ocean Energy Research, National University of Ireland Maynooth, Co. Kildare, Ireland

ARTICLE INFO

Article history:
Received 25 June 2014
Accepted 10 April 2015
Available online 14 May 2015

Keywords:
Met-ocean
Power matrix
Wave energy converter
Long-term
Sea state
Spectrum

ABSTRACT

This paper presents a study of several factors that affect the long-term performance of Wave energy Converters (WECs) based on the methodology presented in de Andres et al. (2013). This methodology consists of a sea state selection technique (MaxDiss), then this selected sea states are introduced into a numerical model in order to calculate the power performance. Finally this data are interpolated with a non linear technique (Radial Basis functions) in order to obtain the long term performance of a WEC on a long met-ocean data series with low computational requirements. In this paper, three types of converter, a one body heaving converter (follower), a two-body resonant converter as well as a deep water flap are investigated. Also four different locations with different met-ocean conditions in terms of the scatter plots and the sea conditions (swell-wind sea) distribution were selected (North of Spain, West of Denmark, Chile and West of Ireland). The methodology worked perfectly for all the selected alternatives, although it was demonstrated to work better for non-resonant converters that are not band limited in their frequency response. Also, the classical method of power production assessment based on the power matrix was reviewed, analysing the analytical spectrum assumption. The influence of more than one peak spectrum on the power production was found to be large on a sea state by sea state basis (±200%) but also on the Annual Energy Production (±40%).

© 2015 Elsevier Ltd. All rights reserved.

1. Introduction

Wave energy converters are still at a prototype testing stage and only few converters have been on open sea conditions for a long period of time. Numerical modelling techniques are popular in order to estimate the performance of a converter on a particular location. Normally the average annual power is computed with the multiplication of the scatter plot (% of occurrences of a set of sea states) by the power matrix (power of the converter on a set of sea states). However, as stated by Ref. [1] this method just provides a figure with the average power production and it is partially inaccurate. Furthermore, when evaluating a particular wave energy converter development from the economic point of view, the interannual variability it is essential to estimate the profitability of a project according to [2]. Then, a methodology to estimate the long term performance of a wave energy converter in a location with low computational requirements it is very valuable tool for WEC development and optimization.

The methodology presented in Ref. [1] assumes that a long met-ocean data series is available with the most important spectral parameters. This methodology consists of a sea states selection techniques in order to separate a subset of sea states from the database that best represents all the database sea states. In this methodology, the MaxDiss algorithm from Ref. [3] is proposed because it represents very well the boundaries of the database in a multidimensional domain. It is based on a selection that computes the distance between points in a multidimensional space and selects the most distant points in order to cover the overall variability of the set.

The power production of these selected sea states is computed with a numerical model and then the whole series of power production is computed with a non-linear interpolation technique, a Radial Basis Functions (RBF) proposed by Ref. [4] used previously in the downscaling of wave climate to coastal areas, see Ref. [5].

In Ref. [1] the methodology was validated with a two-body heaving converter and a location in the North of Spain. However

* Corresponding author. Tel.: +34 942201616.
E-mail address: guancher@unican.es (R. Guanche).

http://dx.doi.org/10.1016/j.renene.2015.04.026
0960-1481/© 2015 Elsevier Ltd. All rights reserved.

it is considered that the investigation of the sensitivity of the methodology to different parameters could be useful for future developments.

Currently there are several types of wave energy converters with different working principles and the power characteristics of several of these are extremely different. Ref. [6] studied eight different types of converters on different locations and as can be concluded from this paper the different mechanic principles of WECs provoke different power matrices. One of the factors that will be studied on this paper is how the different power matrices affect to the methodology and the long term performance of a WEC.

A further consideration, beyond sea state selection and device characterization, is the frequency spectrum of the sea states. When computing the power matrix of a device often an analytic spectra is supposed (i.e. JONSWAP or Bretschneider). However this assumption influences the performance of a WEC and sometimes the real spectra on open sea conditions does not fit with the analytical spectral representation. Some authors, e.g. Refs. [7] and [8] studied how an improved characterization of sea states influence the performance of a WEC. They stated that analytical spectrums are erroneous by 63% due to the existence of sea states with more than one peak. It was concluded that the sea state characterization with analytical could provoke a large error in the power production predictions. With respect the SEAREV device on the SEMREV site they concluded that he analytical spectrum assumption led to an under-estimation of the harvested power by the device.

Also [9] studied the sensitivity of the wave groupiness and spectral narrowness for some wave energy converters. They concluded that the sensitivity of a WEC to spectral bandwidth is more pronounce when the mean period is near the resonance period of the device and also when the response of the WEC is broad . Ref. [10] studied the distribution of the different sea states that occur at the Portuguese coast in terms of number of modes and directionality. Then it is clear that the sea state characterization influences the calculated power performance with numerical models of a converter significantly. Thus, it is clear that the sea state characterization is a key parameter that influences long term power performance of WEC and an accurate approach is needed in order to estima Annual Energy production of WEC.

Also, the met-ocean conditions are very variable and then the scatter plots are changeful. In Ref. [1] a location in the north of Spain was set to develop the methodology. However, as stated in Ref. [1] the broadness and the peakness of the scatter plot influences very much the long term performance of a wave energy converter and it is a parameter that should be studied for future uses of the methodology.

This paper focuses on the influence of the type of WEC, the scatter plot type and the different spectrum data types available in order to define the influence of each aspect on the ultimate power production. Also, the influence of the assumptions regarding the spectral shape on the power matrix will be investigated. Firstly the numerical model used will be explained, secondly the different sets of factors analysed (WEC, location and spectrum data type) will be explain, thirdly the methodology consisting on the set of simulations run will be stated and finally the results will be presented.

2. Numerical model description

The three wave energy converters used in this study were investigated using a common numerical model. The same equation set and computer program was used for each device with different inputs to represent the particulars of each device and its associated power take off equipment. This section will present the common aspects of the equation set and the computer program while the next section will present the device specific inputs and other considerations related to the numerical model and calculations.

The model is a classical frequency domain model as described by Ref. [11]. The equation solved to arrive at the motion of the floating body at each wave frequency is

$$\widehat{u} = \widehat{X}/Z_{mech} \tag{1}$$

where $\widehat{u}$ is the vector of complex amplitude of velocity per unit wave height, $\widehat{X}$ is the excitation transfer function, a vector of complex amplitude of excitation force per unit wave amplitude, and Z_{mech} is the mechanical impedance matrix of the system. Z_{mech} is calculated from

$$Z_{mech} = (m+a)i\omega + (b+b_e) + (c+c_e)(i\omega)^{-1} \tag{2}$$

where m is the inertia matrix of the rigid body, or bodies, composing the system, a is the hydrodynamic added mass matrix of the system, b is the hydrodynamic radiation damping matrix of the system, c is the hydrostatic stiffness matrix of the system, ω is the wave frequency and $i = \sqrt{-1}$. The quantities $\widehat{X}$, a & b are calculated using WAMIT which is one of the commercially available Laplacian flow solvers. b_e and c_e are linear damping and stiffness matrices respectively that together are used to represent the so called "external forces" (due to the device floating in the water). External here is intended to indicate forces external to the hydrodynamic system, these forces include linearized power take off forces and may also include linearized mooring forces, joint reaction forces and fluid pressure forces associated with flow effects neglected by the Laplacian flow solver, namely forces due to viscous effects:

$$b_e = b_{pto} + b_{moor} + b_{joint} + b_{visc} \tag{3}$$

$$c_e = c_{pto} + c_{moor} + c_{joint} + c_{visc} \tag{4}$$

The result of Equation (1) is a velocity per unit wave amplitude, the actual velocity amplitude that results from any given incoming wave spectrum is $(\widehat{a}\widehat{u})$ where $\widehat{a}$ is the wave amplitude which, for unidirectional waves, is calculated from Ref. [12]

$$\widehat{a} = \sqrt{2S(\omega)\Delta\omega}\cdot e^{i\theta} \tag{5}$$

where $S(\omega)$ is the spectral density of the incoming waves at frequency ω, $\Delta\omega$ is the frequency step and θ is a random phase angle uniformly distributed in the range $-\pi \le \theta < \pi$.

The power take off force per unit wave height $\widehat{F}_{pto}$ is

$$\widehat{F}_{pto} = -\widehat{u}b_{pto} - \widehat{x}c_{pto} \tag{6}$$

And the power take off force due to any given input wave amplitude is $(\widehat{a}\widehat{F}_{pto})$.

The average power absorbed by the wave energy conversion device is then calculated from

$$P = \frac{1}{2}\sum_{\omega} |\widehat{a}|^2 |\widehat{u}| \left|\widehat{F}_{pto}\right| \cos\left(\angle\widehat{u} - \angle\widehat{F}_{pto}\right) \tag{7}$$

The position of the system, in addition to the velocity, is also needed. The position per unit wave height, $\widehat{x}$, can be calculated from Ref. [13,14].

$$\widehat{x} = \widehat{u}/(i\omega) \tag{8}$$

The response amplitude operator, a commonly used measure of strength magnitude in hydrodynamics, is $|\widehat{x}|$, the magnitude of $\widehat{x}$. The position amplitude, similarly to the velocity amplitude, is $(\widehat{x}\widehat{a})$.

When the value of $(\widehat{x}\widehat{a})$ is known for a sufficient range of frequencies the variance of the WEC position in a given sea state can be calculated from

$$\sigma^2 = \mathrm{var}(\widehat{x}\widehat{a}) \approx \frac{1}{2}\sum_{\omega} |\widehat{x}\widehat{a}|^2 \tag{9}$$

There is no expression for the maximum position that a WEC will take in any given sea state but given the variance of position, the position with any chosen exceedance may be calculated from an inverse cumulative normal distribution function. We define $x_{n\%}$ as the position where n% of values in the position time series are in the range $-x_{n\%} < x < x_{n\%}$. The implementation of the inverse normal cumulative distribution functions used was the Matlab implementation from Ref. [23]. This knowledge of variance and exceedance values is used to apply relevant constraints to the position in power producing modes of motion, in other words PTO end-stops.

In all the calculations in this paper the reference frequency vector used had 128 equally spaced frequencies with a maximum frequency of π rad/s and a frequency step of $\pi/128$ rad/s.

The above equations were implemented in a Matlab program, in execution for each device in each sea state the computer program used a simplex optimization algorithm to manipulate the power take off damping (and optionally stiffness) to minimize $-P$ subject to the constraint that the $x_{98\%}$ exceedance value is less than a specified maximum. The results is that in most smaller sea states the optimum damping is chosen but in larger sea states higher damping values than those that correspond to maximum power are sometimes chosen by the optimization in order to limit the extreme positions.

3. Description of the studied parameters

3.1. WEC device types

Three different wave energy converters (WEC's) were studied in this paper. These devices were firstly a heaving buoy with bottom reference, secondly a two body heaving buoy with power production in relative heave, and lastly a deep water hinged flap with power take off in pitch. These devices are generic and are not related to any particular commercial design, but the relevance of these generic devices is bourne out by the many devices that have been proposed and/or promoted that are conceptually close to these generic devices. Real world devices operating on similar principles to WEC 1 include [14] and [13] as well as many others, devices operating on similar principles to WEC 2 include [15] and [16] and devices operating on similar principles to WEC 3 include [17] and [18]. Representations of the geometries used are given in Fig. 1 and the geometrical parameters are summarized in Table 1. It should be noted that in WEC 2, Body 1 is the outer toroidal float and Body 2 is the central cylindrical spar with circular heave plate at its lower end. Both of these bodies are surface piercing, and have equal freeboard.

The linear hydrodynamic properties of the three devices were calculated using WAMIT, the solution to the Radiation problem is presented in Fig. 2 and the solution to the diffraction problem is presented in Fig. 3. In all three graphs the ordinate is normalized by dividing each curve by its maximum value, these maxima are presented in Table 2. WEC 1 and WEC 3 are single degree of freedom systems so the equations and hydrodynamic coefficients are scalars. WEC 3 is a two degree of freedom system so the radiation damping and added mass are 2 × 2 matrices with frequency dependant elements. The frequency dependence of the main diagonal of these matrices is plotted in Fig. 2 (WEC2-B1 & WEC2-B2).

The power take off machinery was represented by the matrices b_{pto} and c_{pto} as introduced in the previous section. For all three devices c_{pto} was set to zero, i.e. the power take off force was assumed to be purely linear damping with no stiffness component. The value of b_{pto} is calculated from

$$b_{pto} = b\Pi \tag{10}$$

where b is a scalar damping coefficient and π is a pattern matrix. In our case b is a trial value supplied on each iteration by the optimization while the pattern matrix is a device specific constant. For WEC1 and WEC3 the power producing modes of motion coincide with the axis of the co-ordinate system so that by suppressing the non-power producing modes of motion the equations are reduced to a scalar equation and $\Pi = 1$. For WEC 2 the power production is in relative heave, the equations are reduced to 2 × 2 dimension (heave of body 1 and heave of body 2) and the PTO pattern matrix is set to

$$\Pi = \begin{bmatrix} 1 & -1 \\ -1 & 1 \end{bmatrix} \tag{11}$$

The motion of each device was constrained using the methodology introduced in the previous section. The constraints for the each WEC are summarized in Table 3.

The power matrices that result from this calculation are given in Fig. 4. These power matrices have been populated with JONSWAP spectra with gamma 3.3 of the sets H_s and T_p that appear on the figure axis.

WEC1 shows a low response in sea-states with peak periods below its natural period in heave and a wave follower behaviour in sea states with peak periods above its natural period (wave follower means that amplitude and phase of body motion approach wave amplitude and phase). This behaviour is consistent with the shape of the excitation force curve and the arrangement of absolute PTO reference. WEC1 behaves as a low pass filter, it responds equally well to all frequencies below its natural frequency and does not respond well to higher frequencies. In addition, in panchromatic seas WEC1 does not demonstrate significantly higher power near its natural frequency than it does at lower frequencies. Therefore, even though WEC1 is strictly capable of heave resonance we classify it as non-resonant since the resonance does not significantly aid power absorption.

WEC2 shows a peak power absorption in sea states with peak periods of approximately 9 s with lower absorption at higher and lower periods. The peak at 9 s corresponds to the natural period of the device in the 'locked bodies' condition. The power increases with period up to this point and after this point the decrease in power is related to decreasing phase angle of the relative heave motion of the two bodies in the device. At very large periods the two bodies will move together as wave followers (motion amplitude and phase of each body approaching wave amplitude and phase). Since WEC2 only extracts power well at frequencies near its heave natural frequency therefore we classify it as a resonant device.

WEC3 the power peaks in sea-states with peak periods of about 6 s. Unlike WEC2 this peak is not related to the natural period of the device but to the wave forces which have a maximum in this period range. The natural period of the flap in pitch about an axis on the sea floor is in fact much longer than 6 s. The wave forces indicated for WEC3 by the excitation and radiation damping curves in Figs. 2 and 3 peak at approximately 5 s. Since the power absorption of WEC3 at its natural frequency is much lower than its maximum power absorption we classify this as a non-resonant device.

It needs to be clarified that in this piece of research, for the sake of simplicity only unidirectional spectra have been considered. In

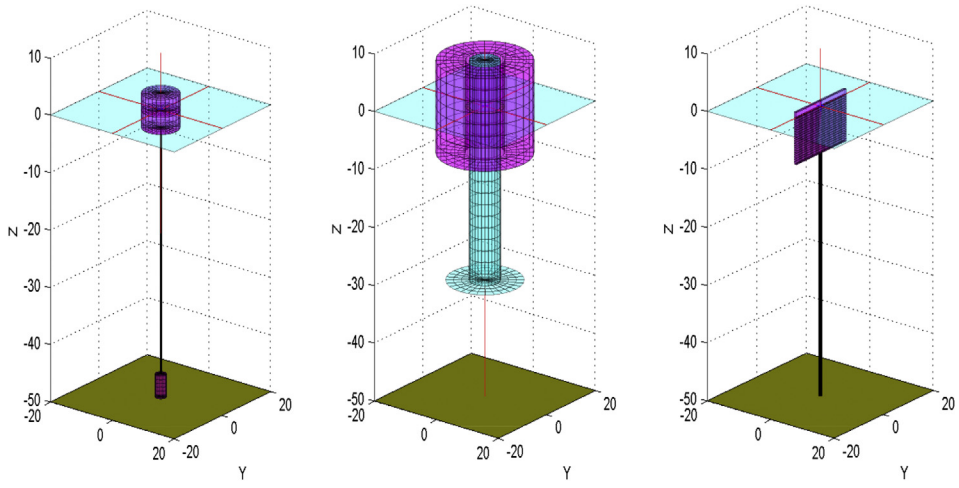

Fig. 1. Geometries of WEC1, WEC2 & WEC3: Single body heaving buoy, two body heaving buoy and a deep water pitching flap respectively.

Table 1
Summary of principal geometrical parameters of WEC1, WEC2 & WEC3.

WEC 1			WEC 2			WEC 3		
Diameter	10.0	m	Torus OD	25.0	m	Width	20.0	m
Draught	3.0	m	Torus ID	10.0	m	Draught	8.0	m
Freeboard	3.0	m	Torus Draught	8.0	m	Thickness	0.7	m
			Column OD	8.0	m	Freeboard	1.0	m
			Plate OD	20.0	m			
			Column Draught	30.0	m			
			Freeboard	8.0	m			

this study the influence of the broadness (multi-peak) of the spectra is analysed in the methodology presented in de Andres et al. (2013). The addition of the wave direction as a parameter on this methodology will be carried out on future research, because it is known that in WECs such as the flap, its influence on the performance is extremely high.

3.2. Location

Four different locations are selected for this study. These locations have very different characteristics due to the different position around the globe and the different atmospheric dynamics that are governing them. Ian Fig. 5 the locations are shown on the globe map. The locations are North of Spain (Bilbao, near BIMEP), North-West of Denmark (near Hanstolm), West of Ireland and South-Central Chile.

In Fig. 6 the scatter plots of the locations are shown (percentage of occurrence over time). Bilbao location is characterized by a scatter plot concentrated around 9 s and with relatively low wave heights. Denmark is characterized by low peak periods and a very concentrated scatter plots around low wave heights. On the other hand, Ireland has a very broad scatter plot characterized by very energetic sea states, with high wave heights and peak periods around 10 s. Chile has an extremely concentrated scatter plot with quite high peak periods and wave heights around 2.5 m.

Also, an investigation about the sea state type on each location has been performed based on the number of peaks of the spectrums and on the type of component (swell and sea). This separation of the components has been performed based on the steepness method proposed by Ref. [19] computing a separating frequency when distinguishing between wind sea and swell based on the moments of the spectrum.

Fig. 7 represents the sea state distribution on the different locations. Firstly, in Bilbao there are almost 50% of one peak sea states (42% swells and 6% seas), the 50% left are combined sea states with a predominance of swell + sea states. In Denmark, the percentage of one peak sea states is lower (around 45%, 15% of swells and 30% of seas). However the percentage of more than one peak is quite high (around 65% having 30% of sea + swell sea states).

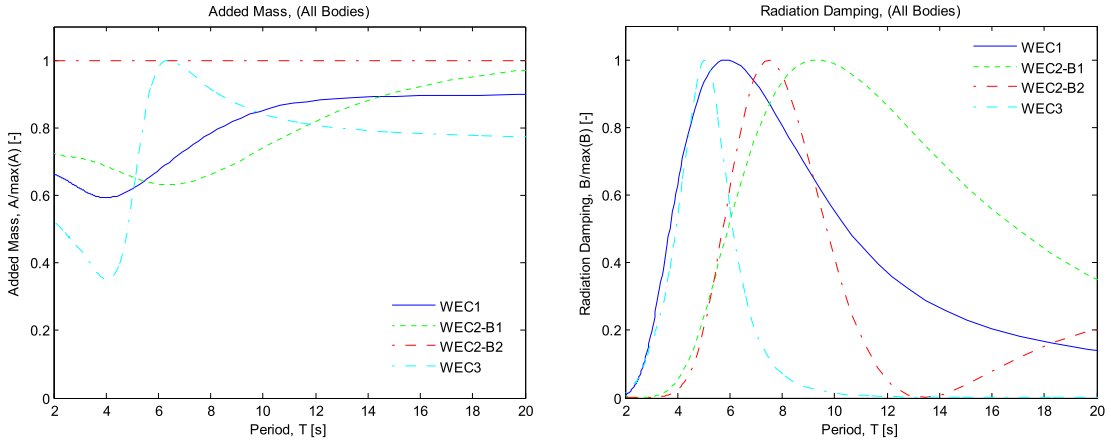

Fig. 2. Added mass and Radiation damping for all devices. WEC2-B1 & WEC2-B2 refer to WEC2 Body 1 and Body 2 respectively. (Off diagonal cross-coupling terms in the multi-body WEC 2 are not shown). Scales are normalized see Table 2 for more information.

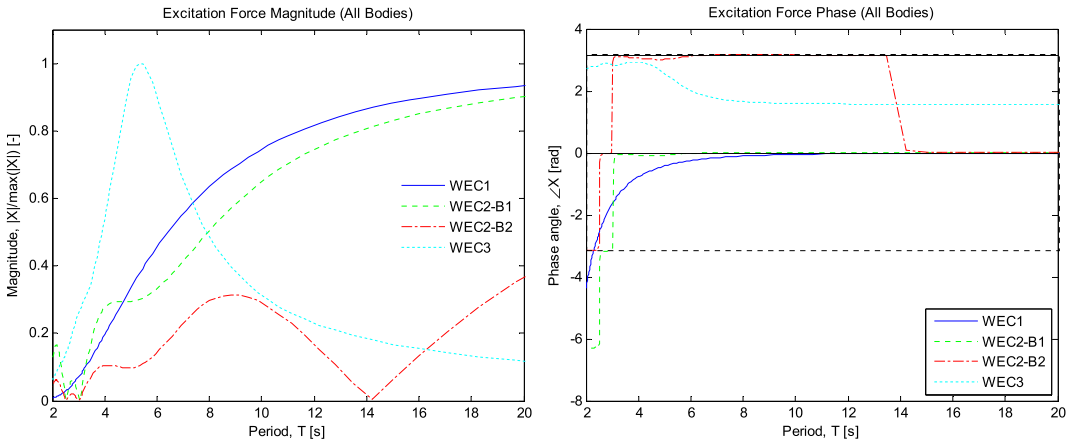

Fig. 3. Excitation force transfer function for all devices. WEC2-B1 & WEC2-B2 refer to WEC2 Body 1 and Body 2 respectively. Magnitude is normalized see Table 2 for more information.

On the contrary Ireland is the location with the highest percentage of swells (around 40%) and the number of sea states with more than 1 peak is quite low (around 40% with 20% of swell + sea states). Also, Chile is similar to Ireland in the sea state distribution with almost 60% of sea states with a single peak and the remaining 40% with more than one peak.

3.3. Data type

For this study four different data types have been selected. However not all the data types are available for all the locations. Buoy data was available just for the Bilbao location. This buoy corresponds to the buoy located off Bilbao port. It is located on the coordinates 3,05° West and 43,64° N, on a depth of 600 m and it has spectral hourly data from 2009 until today.

The second data source is the IFREMER spectral data base, available for all the locations. This database has a 0.5° resolution grid, 3-h time step, homogeneous and continuous that covers the years 1994–2012 [20,21]. This database splits the spectrum into individual wave fields (1 sea and 5 swells) using the method of [22] as described in Ref. [23]. The selected points in this database are less than 100 km distant from shore and less than 200 m deep. The use of this database provides smoothed spectrums of more than one peak on the selected locations. For this IFREMER data base the spectrums are available from 1993 to 2012. These sets then account for 58.440 sea states. For the Bilbao location the coincident dates between the buoy data and the IFREMER data base were taken. These dates are from 2009 until 2012 with a 3 h span, what accounts for 9469 sea states.

When simulating the performance of WECs some analytical spectrum such as Brechdneider, JONSWAP or Pierson Moskowitz are used because they are very similar to a perfect swell sea state. Normally JONSWAP spectrum is one of the most used. This spectrum has a peak enhancement factor called γ that is usually set to 3.3, however it could be changed from 1 (typical for wind seas) to 7 (typical of long Atlantic swell).

The third set of data in this study consists of the JONSWAP spectrums with the same wave height (H_{m0}) and the same peak period (T_p) as the IFREMER data. The fourth data set consists of JONSWAP spectrums with the gamma parameter chosen to give a best fit to the IFREMER sea states. It should be pointed out that the same wave height and peak period are maintained in order to compare the different spectral representations.

For the Bilbao location 4 data sets will be used, on the other hand for the rest locations 3 data sets will be used. It should be pointed out that the buoy location does not match perfectly the IFREMER data points and then an interpolation between two IFREMER data points was taken for comparison with the buoy data in order to reduce the spectral errors due to shoaling and refraction.

One of the aims of this paper is to analyse the influence of the one peaked spectrum assumptions on the final power of the device. Fig. 8 shows two examples for the different selected data sets of how one peak spectrums fit to real spectrum. In the left panel a spectrum from the IFREMER data base (red (in the web version)) is compared with a JONSWAP spectrum with gamma 3.3 for the same H_{m0} and the same T_p. It should be noticed how the JONSWAP spectrum only fits with the swell component and not with the wind sea peak. On the right panel the four different data types for the Bilbao location are represented. Here the blue line represent the buoy data, while the green line represents the IFREMER data. As it can be seen the correspondence is very good and the IFREMER data pick the two spectrum peaks. With the red dotted line and the black dotted line the JONSWAP with gamma 3.3 and the best gamma fit respectively are represented. As can be seen in this spectrum the JONSWAP fit does not represent correctly the multi-peaked or multi component nature of the measured spectrum. The influence of this fact on the power production assessment will be investigated.

Table 2
Maximum values used to normalise the curves in Figs. 2 and 3.

	A (N)	B (Nm)	|X| (m)
WEC1	3.395×10^5	7.627×10^4	7.827×10^5
WEC2-B1	3.464×10^6	5.443×10^5	4.108×10^6
WEC2-B2	2.606×10^6	2.950×10^3	4.987×10^5
WEC3	2.790×10^7	2.011×10^7	7.113×10^6

4. Methodology

4.1. Selection and interpolation methodology

As explained in the introduction, this paper continues the work explained previously in Ref. [1]. The methodology used to obtain the long-term performance of a wave energy converter consists firstly of a sea state selection technique, secondly of calculation of power production in those selected sea states and thirdly of

Table 3
Position constraints applied to damping optimization.

	$x_{98\%}$	Units	Mode
WEC1	2.0	m	Heave
WEC2	4.0	m	Relative Heave (B1–B2)
WEC3	0.3	rad	Pitch

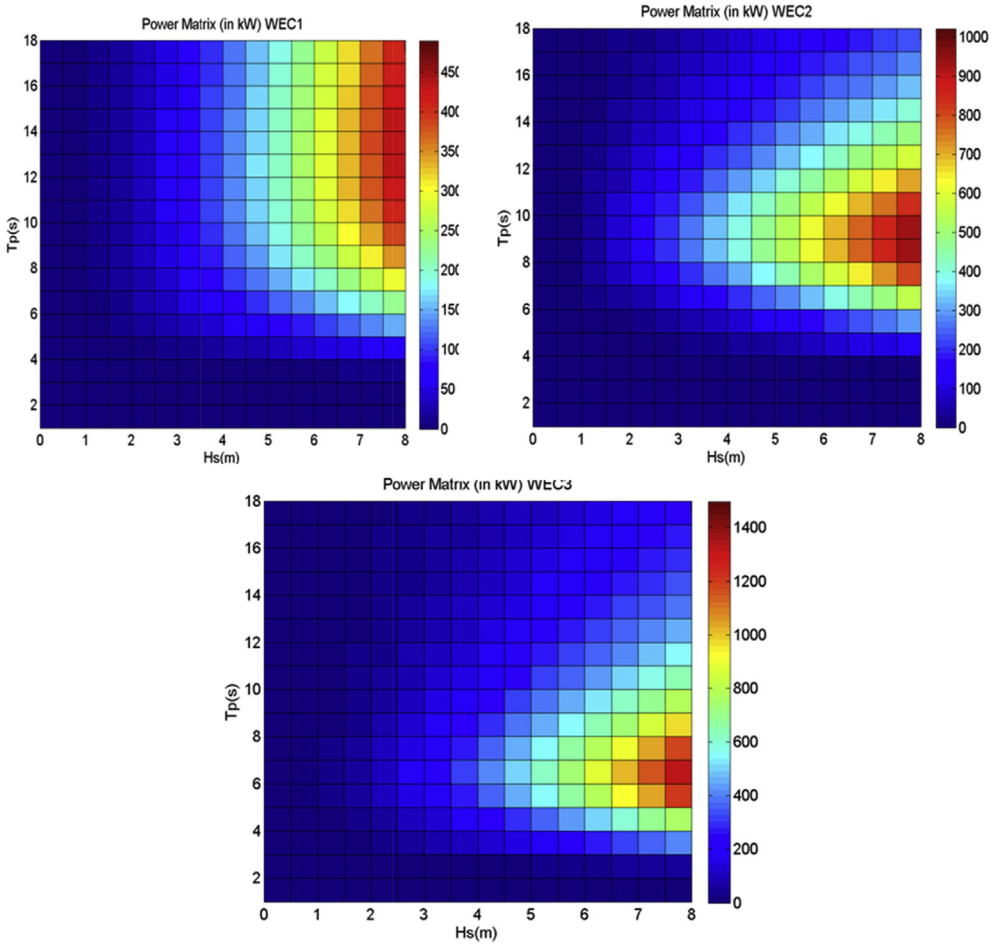

Fig. 4. Power matrices of the considered WECs.

application of a non-linear interpolation using radial basis functions to give power estimates for any required sea state not limited to the selected sea states. The sea state selection technique is used to extract a representative subset of sea states from the database.

In this methodology, the MaxDiss algorithm from Ref. [3] is proposed for the sea state selection step because it represents very well the boundaries of the database in a multidimensional domain. It is based on a selection that computes the distance between points in a multidimensional space and selects the most distant points it order to cover the whole variability of the set.

In Ref. [1] the selection technique was applied over the parameters H_s and T_p because in that paper the spectrums were

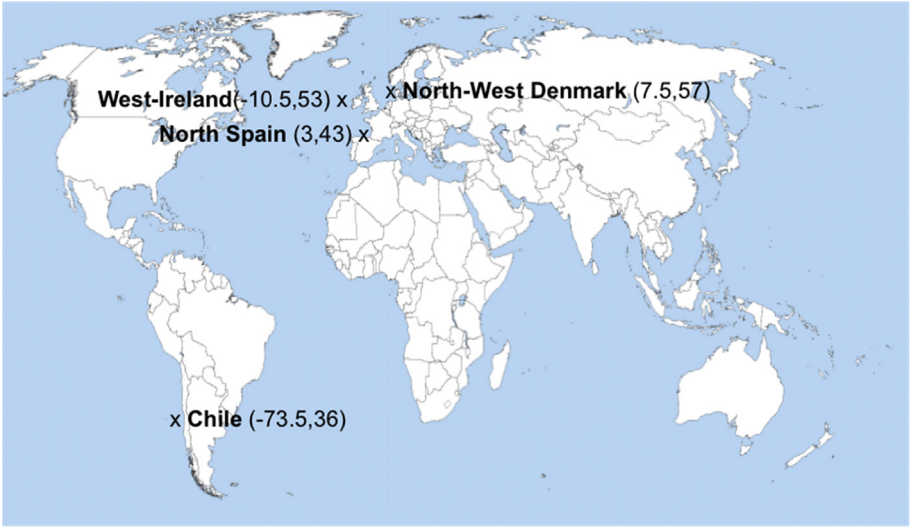

Fig. 5. Map with the selected locations (latitude, longitude).

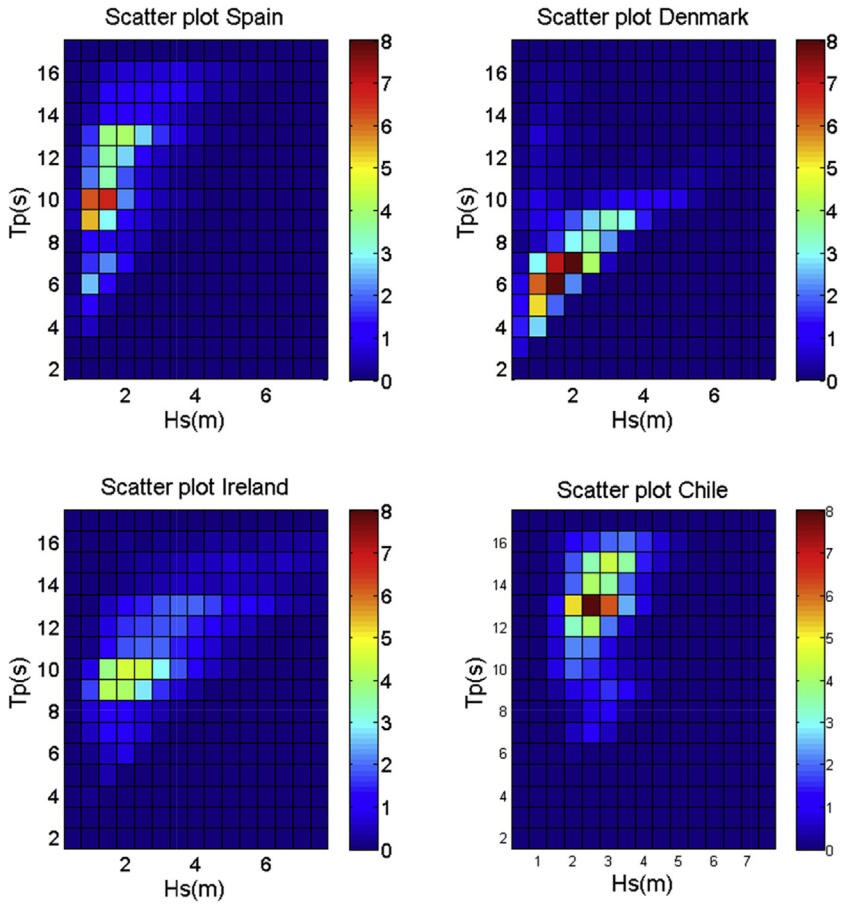

Fig. 6. Scatter plots in percentage of the selected locations (data from IFREMER database).

assumed to be JONSWAP and 2 parameters was enough to characterize the sea states variability.

For this paper a selection approach based on three parameters is chosen due to the fact that the spectrums are not single peaked and a parameter relating to the shape of the spectrum is needed. From Ref. [9] it was concluded that the parameter ε_0 is well suited for representation of the peakness and broadness of the spectrum. In Ref. [8] it was also found that the parameter ε_0 is strongly correlated with the device production and capture width.

$$\varepsilon_0 = \sqrt{\frac{m_0 \cdot m_{-2}}{m_{-1}^2} - 1}$$

This parameter measures the peakness and broadness of the spectrums. A set of real spectrums from the Bilbao buoy set was analysed, each sea state was identified as single, double or triple peaked and the value of ε_0 was calculated for each sea state, the mean and standard deviation of ε_0 was calculated for each category of peakness. In Fig. 9 the wide columns give the mean values and the error bars give ±1 standard deviation. It is evident that the single peaked sea states have a lower mean value of ε_0 and a much lower standard deviation.

For this study a sea state selection based on H_{m0}, T_p and ε_0 was computed. The whole data set used consisted of 58,460 sea states for the Ireland, Chile and Denmark locations and 9469 sea states for the Bilbao location. In Fig. 10 a selection of 100 sea states are represented over the whole set of sea states. The colorbar (in the web version) represents the value of the ε_0 parameter. As it can be seen this methodology selects the most different and distinct sea states with respect to the three chosen parameters H_{m0}, T_p and ε_0. In all the plots it could be seen how the sea states with higher ε_0 accumulates generally on the area with low wave height. This is due to the fact that combined sea states of swell and wind sea correspond to sea states with generally low energy while the states with the largest amount of energy correspond to perfect swells.

After the selection process, the power production of this selected sea states is computed with a numerical model in this case a frequency domain calculation as described in Section 2 and then the whole series of power production is computed with a non-linear interpolation technique, Radial Basis Functions (RBF) proposed by Ref. [4] used previously in the downscaling of wave climate to coastal areas. After this non-linear interpolation technique the power production series along the time where the met-ocean conditions are known is computed. The result with the different data sets will be explained in the next section.

4.2. Simulation sets

One of the aims of this paper is to make a comparison between an exhaustive evaluation of all available sea states and an evaluation based on selected sub sets of these sea states. This comparison considers both computation time and accuracy of the result.

For Ireland, Chile and Denmark power production of each device in the 58,460 sea states from the IFREMER database and JONSWAP spectra fitted to these were all evaluated. For Bilbao the same was done but with 9469 sea states and with the addition of the dataset from buoy measurements. This exhaustive calculation of all sea states is regarded as the best possible estimate of power production

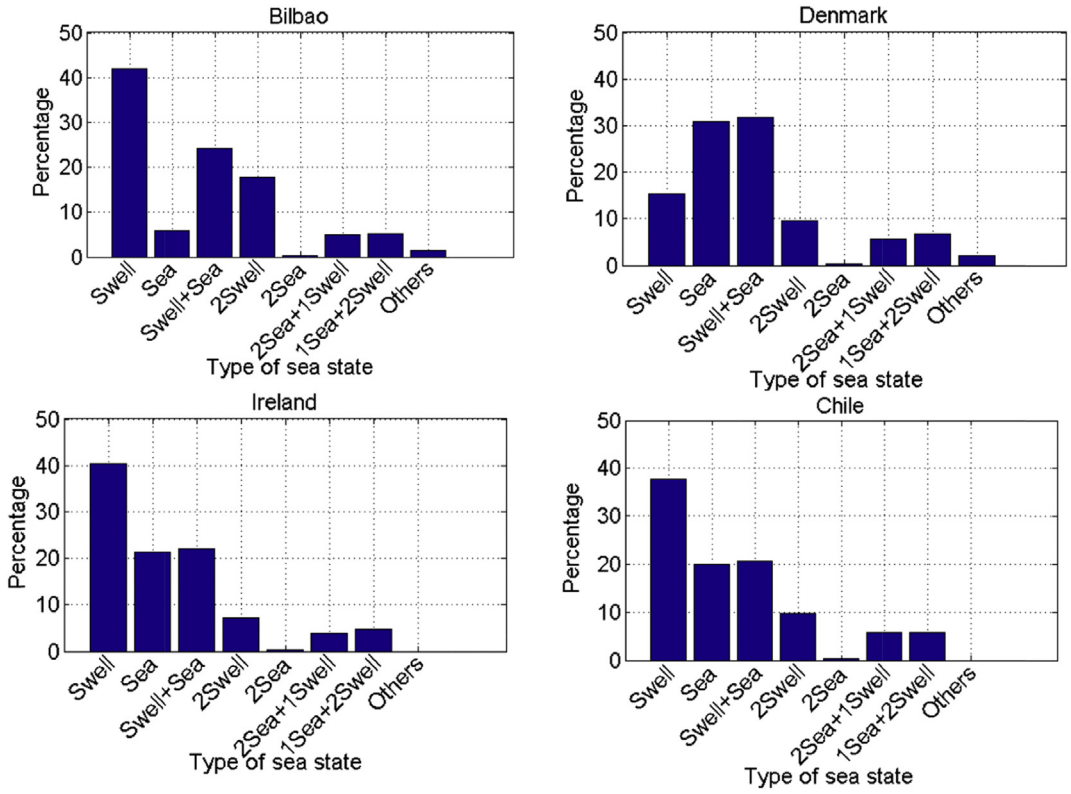

Fig. 7. Sea state distribution (% in time) over the studied locations.

of the selected devices from the given data and the quality of estimates based on selected subsets of se states may be gauged by comparison (Table 4).

Several subsets of the sea states of different sizes were evaluated, these were 100, 500, 1000 and 2000 sea states. Table 5 gives a summary of the combinations of devices, locations, sea state characterisations and sea state subset selection size that were evaluated. Ultimately, for the Ireland, Chile, Denmark locations the annual energy yield for each device was assessed using 15 different wave resource descriptions (3 sea state characterisations $\times$ 5 sea state selection sizes) and for Bilbao the annual energy yield for each device was assessed using 20 different wave resource descriptions (4 sea state characterisations $\times$ 5 sea state selection sizes).

5. Results

In Section 5.1, in order to compare results calculated from the whole data set with results calculated from selected sub sets the results of the select-evaluate-interpolate methodology will be presented for the three devices in the Bilbao location with all sea state characterizations (buoy, IFREMER, JONSWAP $\gamma = 3.3$ & JONSWAP $\gamma =$ best fit).

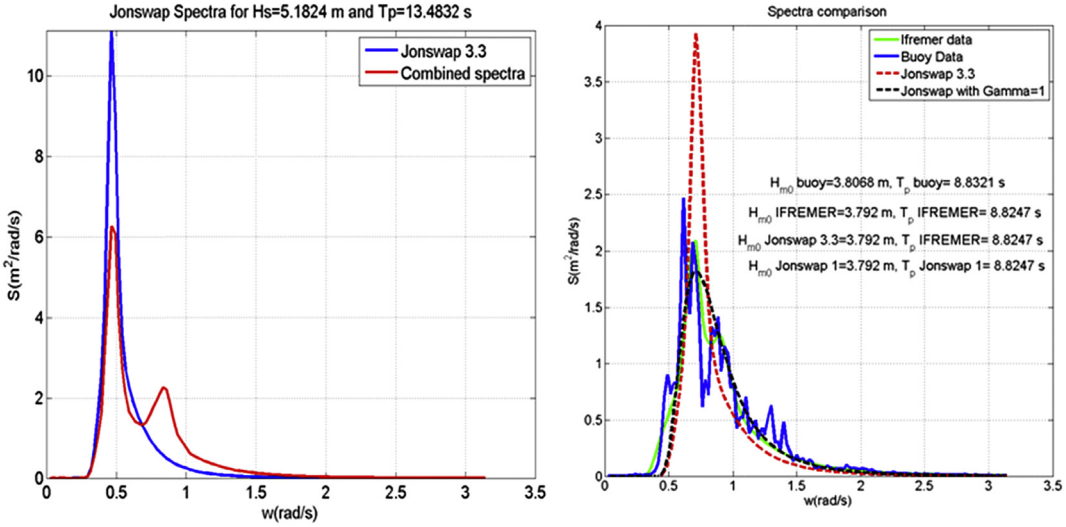

Fig. 8. Different data types selected, at Bilbao location.

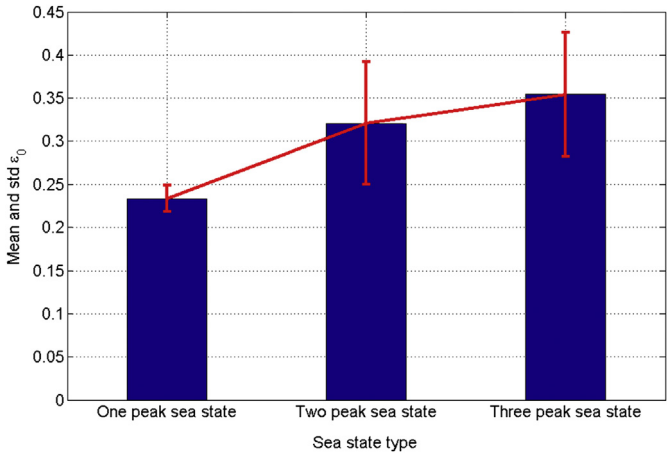

Fig. 9. Peakness of the spectrums based on ε_0.

In Section 5.2 the effect of sea state characterization (spectral shape) on the power production of each device in each location is investigated by comparison of annual energy production calculated from each sea state characterization.

5.1. Long term power results

In this first subsection the results of the long-term power production assessment with the different data sets proposed in the previous sections are presented. As explained on the previous subsection, for all the sets the whole number of sea states is run and also the cases with the selected sea states in order to compare the performance of the select-evaluate-interpolate methodology with the exhaustive evaluation.

In Fig. 11 the "best estimate" of power on the y axis (obtained from running the whole set of sea states) is plotted against an estimate of power reconstructed by interpolation between the 100 selected sea states for the Bilbao location for the buoy data. Here the power of the set of 9469 sea states for both real and reconstructed power are represented. In this case it can be seen that the correspondence between real and interpolated data is very good. The correlation coefficient is 0.98 and the scatter index is 0.02. The scatter index represents the spreading of the data with respect the real data. In this case is very low, that means that correspondence is excellent. Then we can conclude that applying the MaxDiss selection technique we can represent the variability of the whole set of sea states and with the interpolation technique it is possible to approximate the power production on a long-term series with very low computational effort.

Table 4
Summary of role of resonance in power absorption and of qualitative description of frequency response for three WEC.

WEC	Power absorption mainly through hydrodynamic resonance	Qualitative description of frequency response
1	No	Low pass filter (Device is a wave follower)
2	Yes	Band limited (Due to heave resonance)
3	No	Band limited (Due to band limited nature of input diffraction/excitation forces, see Fig. 3)

This procedure is followed for the whole set of cases and then the reconstructed power is compared with the power computed by running the whole sea states series. In Fig. 12 the correlation coefficient of the series with respect the real power obtained by the running of the whole set of sea states (9860 sea states) is represented with respect the number of selected sea states for reconstruction. Blue (in the web version) and red lines correspond to the buoy data and the IFREMER data. Also this fact proves that the selection with respect H_s, T_p and ε_0 is good in order to reconstruct the power of real sea states. Also the r^2 coefficient is higher than 0.97 for 500 cases so it can be concluded that this number of cases is acceptable in order to get an acceptable reconstructed series.

It might be expected that the correlation coefficient should increase with the selection size, the fact that this is not the case for the JONSWAP spectra requires explanation.

However the pink and green lines represent the JONSWAP spectra with gamma 3.3 and best gamma respectively. As can be seen both lines are at lower values as the number of cases increase.

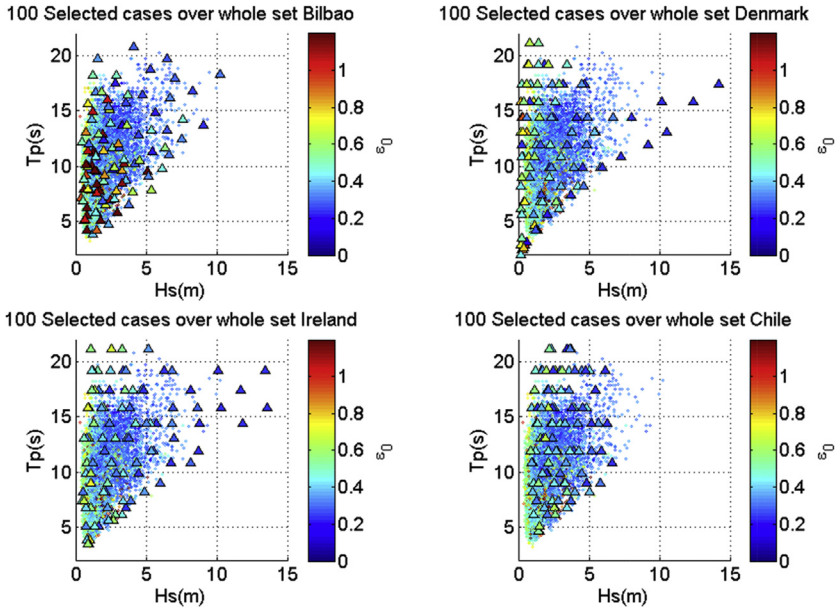

Fig. 10. MaxDiss for 100 selected sea states for the four locations.

Table 5
Data sets for the simulations.

	Location	Data type	Data size
WEC	Bilbao	Buoy data	100
		Ifremer data	500
		JONSWAP 3.3	1000
		JONSWAP best γ	2000
			Whole set 9469
	Denmark		100
		Ifremer data	500
		JONSWAP 3.3	1000
		JONSWAP best γ	2000
			Whole set 58460
	Ireland		100
		Ifremer data	500
		JONSWAP 3.3	1000
		JONSWAP best γ	2000
			Whole set 58460
	Chile		100
		Ifremer data	500
		JONSWAP 3.3	1000
		JONSWAP best γ	2000
			Whole set 58460

This fact means that the selection is not very good for one-peak spectrums because the inclusion of the epsilon parameter within this cases masks the other important parameters (and the good selection). The epsilon parameter is good when treating with real sea states of more than one peak because this parameter takes the broadness of the spectrum. However when treating with analytical spectrums of just one peak the parameter epsilon 0 is not good for sea state selection. This is demonstrated with the dotted black line in Fig. 12 left bottom panel. This line corresponds to the JONSWAP 3.3 spectrums but with the selection taking just into account H_s and T_p (as considered previously in Ref. [1] for one peak spectrums). As can be seen with this selection the goodness of the comparison increases as the number of cases gets higher. Then, it is demonstrated that the MaxDiss selection procedure with 3 parameters is fine in order to represent real spectrums of more than one peak. However when selecting the representative sea states of a one peaked sea spectrums the selection process should be made with just 2 parameters.

WEC 2 and 3 both have band limited response, meaning that the power is high is a certain frequency band and rapidly decays to zero at both higher and lower frequencies outside this band, (WEC2 is band limited due to the band limited nature of its heave resonance and WEC3 due to the band limited nature of its diffraction force)

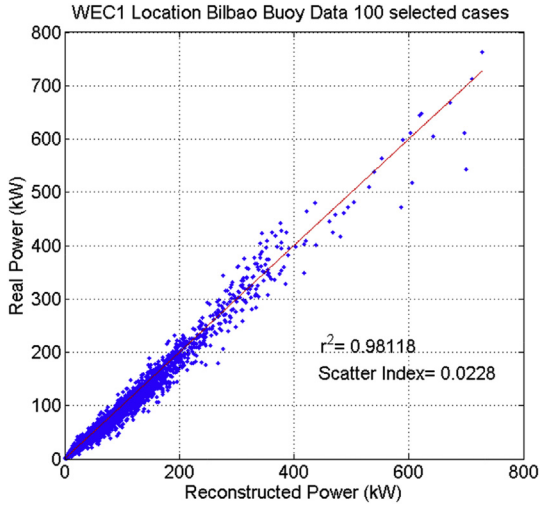

Fig. 11. Comparison between the Real power and the reconstructed power.

consequently the power matrix shows a rapid reduction in power at sea states away from the one with the peak power. WEC 3 has a little bit higher r^2 for the lower number of cases. This is due to the sea state selection because a lot of points are found on the 6 s area due to the existence of more bimodal sea states on the lower periods area.

When comparing the different WECs the WEC 1 is the WEC that gets higher r^2 for all the number of cases. This is due to the smooth slope of the power matrix. WEC 1 is a follower and the power matrix is quite smooth in the peak period axis because it does not rely on resonance for power absorption. Then, it is logic that WEC 1 achieve the highest r^2.

However, it can be concluded from these previous figures that the methodology works well for the different types of converters and the different scatter plots and data type. It is concluded that a lower number of sea states is needed in order to achieve good r^2 for follower WECs. It is also seen how the sea state selection process works well for the real sea states with 3 spectrum parameters and how the representation of the spectrum variability is easily handled with this methodology. In general, with 500 cases the goodness of the fit is very good and then the computational time in order to obtain the whole power production on a long-term basis is much reduced. For instance computing the power of the 500 selected sea states and doing also the non-linear interpolation lasted for 2 h while the whole set of 9469 sea states lasted for 1 day.

5.2. *Influence of spectral shape on power production*

In this section the three WEC's and the four data sets (buoy, IFREMER, JONSWAP with gamma 3.3 and JONSWAP with best gamma fit) will be compared in terms of the power production. In Section 5.2.1 the influence of the spectral shape on the power production is illustrated. The power production of the three selected WEC's in the real non-standard spectra in the IFREMER data is compared to the power of the same WEC's in equivalent JONSWAP spectra.

One of the objectives of this paper was to demonstrate how the assumptions inherent in the classical method of power production assessment influence the power production. By classical method of power production assessment we mean the summation of products of scatter diagram occurrences and power matrix powers. In Section 5.2.2. a comparison is made, for the three selected WEC's, between the classical method and an exhaustive evaluation of all sea states in the IFREMAR data set and also with the two parameter and three parameter JONSWAP spectra fitted to the IFREMAR data.

5.2.1. *Comparison on a sea-state by sea-state basis*

For this case a set of sea states with a combination between swell and wind sea has been selected. In Fig. 13 the selected spectrums for comparison are shown. This set of spectrums correspond to the Denmark location and they are dated between the 12-3-1996 and the 15-3-1996. The data compared here are the IFREMER data base and the two JONSWAP approaches. The IFREMER data is represented in blue and the JONSWAP with the best gamma is represented in pink. As can be seen this period of time is a combination of swell + sea that starts with a more predominant swell, continuing with a more important wind sea and it finishes with a perfect swell.

The power production on this range of time was computed with the different sets afore mentioned and it is shown in Fig. 14. In blue the IFREMER data, in red the JONSWAP with gamma 3.3 and in black the power with the best gamma. As can be seen in the figure the difference between the different series is higher on the first period of time. This first period of time is characterized by a predominant swell firstly and afterwards by a predominant sea. The

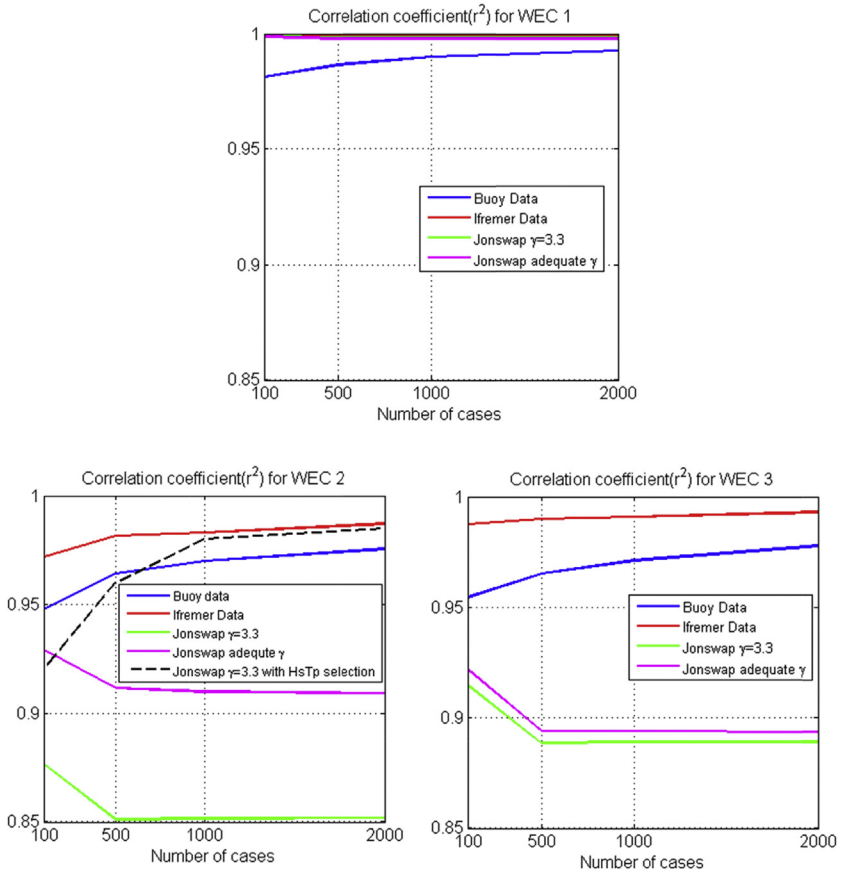

Fig. 12. r^2 coefficient for the different cases for Bilbao (Spain).

differences obtained by the IFREMER DATA (bimodal) and the JONSWAPs are quite high in this first period. For instance for WEC 1 the power obtained by the bimodal sea states is 14 kW and on the other side the power obtained by the JONSWAP spectra is 26 kW, that corresponds to a 85% of difference. This fact highlights the importance of taking into account bimodal sea states because from the isolated point of view the difference between considering real and analytical spectrums is very high.

Analysing the different WECs the highest differences appear for WEC 2. In the first period the difference of the bimodal spectra and the JONSWAP ones are 100%. The JONSWAP spectrums overestimate the power production for the first and second WECs. When the sea states changes to a one peaked sea states on the 15-3-1996 at 6 h the correlation between the different series is much better and the correspondence is much higher.

In Fig. 15 the capture width ratio of the three WECs is represented for the period of study versus the ε_0 parameter for the 3 different met-ocean data considered. The capture width ratio represents an efficiency of the power conversion with respect the incident wave resource. It is calculated according to the next formulae:

$$CWR(\%) = \frac{Power\ absorbed\ by\ the\ device(\mathrm{kW})}{Wave\ Resource\left(\frac{\mathrm{kW}}{\mathrm{m}}\right) * Device\ working\ dimension(\mathrm{m})} \quad (12)$$

In Fig. 15 the IFREMER spectrums are represented with blue (in the web version) dots and the JONSWAP with gamma 3.3 and best fit with red and green dots respectively. As can be seen the bimodal spectrums have values of the ε_0 between 0.2 and 0.7, however the JONSWAP spectrums have very low and narrowly spread values because the broadness of single peaked spectrum is limited. A clear result is that there is a negative correlation between the ε_0 of the IFREMER data and the capture width ratio of the WEC's, that is the devices perform less well in broader sea spectrums.

These extreme points, high ε_0 low capture width, are not well represented by the JONSWAP spectrums and then they may be underestimated or overestimated in this cases.

It is also important to highlight how the blue data points from IFREMER data base have a descending tendency as the ε_0 increases for all the WECs. It means that as the spectrum gets broader and peakier the efficiency of the conversion is lower. This result makes sense because generally the converters are designed to be tuned with a specific period and when the spectrum is broader the converter is not able to capture all the energy of the spectrum. Also, if the three plots are compared it can be seen that blue dots have an approximate slope of -11 (% per unit of broadness), the WEC 2 -104 and the WEC 3 -66.6. It is concluded that the influence of the broadness of the spectrum has a higher influence on the band limited converters (WEC 2 and 3) than in the wave follower converter (WEC 1). This is expected as the wave follower converter has a similar performance for a large range of periods and on the other hand the band limited converters have a much narrower performance for a small range of frequency/periods. (WEC 2 is frequency band limited due to its resonant response, WEC 3 is frequency band limited not due to resonance but only due to band limited nature of its hydrodynamic forces).

In Fig. 16 the comparisons between the IFREMER data base (on the x axis) and the JONSWAP with $\gamma = 3.3$ are plotted. Each point represents a sea state from the IFREMER data set, points to the left and above the red line (in the web version) that bisects the graph

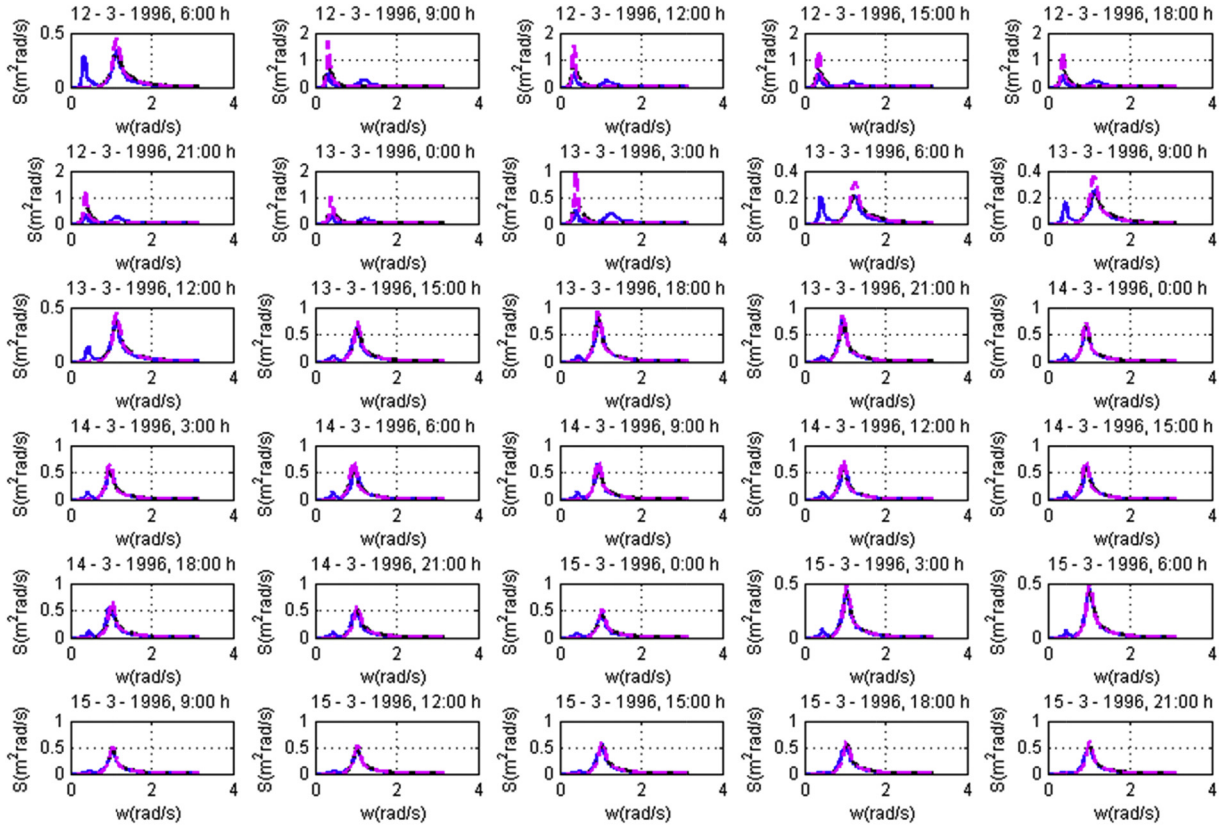

Fig. 13. Set of spectrums selected for comparison IFREMER: blue. JONSWAP (gamma = 3.3): pink. JONSWAP (gamma best fit): black. (For interpretation of the references to colour in this figure legend, the reader is referred to the web version of this article.)

are sea states where the JONSWAP spectra results in an overestimate of the power when compared to the real spectra and points that are below and to the right of the red line are sea states where the JONSWAP underestimates the power. The colorbar represents the broadness of the sea state that corresponds to the power represented with the dots.

As can be seen Denmark is the location where the correlations is lowest for all the devices (the r-squared parameter is 0.99, 0.87 and 0.71 for WEC 1, WEC 2 and WEC 3) respectively. This result was expected as Denmark was demonstrated to have just 40% of one-peaked sea states. Also it can be seen how the points that are further from the bisectrix are the ones with higher ε_0. This is also expected as the broader the spectrum the larger the error when assuming analytical spectrums. It can be also highlighted that theWEC with lower correlations is WEC 3 (as well as WEC 2) because both have a peaky response and then it is more affected by the spectrum broadness. Also, WEC 3 correlation is a little bit lower than WEC 2 because WEC 3 is tuned for a period near 6 s and the broadest spectrums are usually found on this area (see Fig. 10).

WEC 1 is the one with highest correlation for all locations. As explained before this is expected as WEC 1 is a wave-follower and its performance is not as strongly dependant on the spectral shape as is the case for the other WEC's.

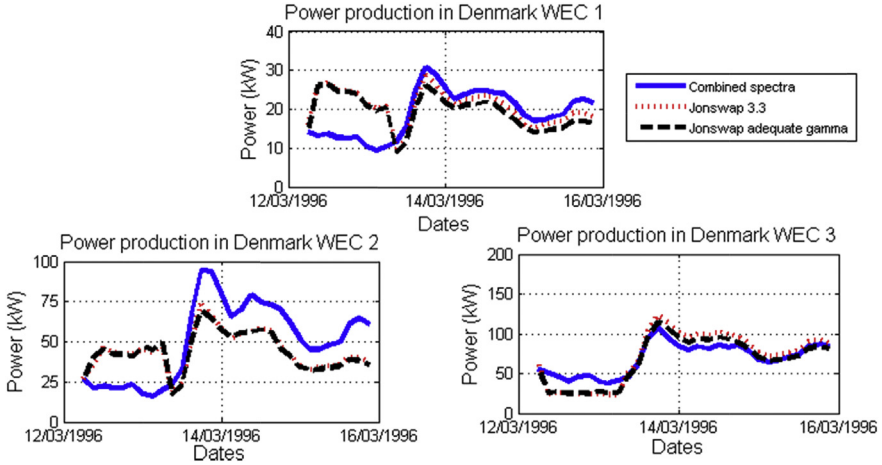

Fig. 14. Power production for the selected spectrums.

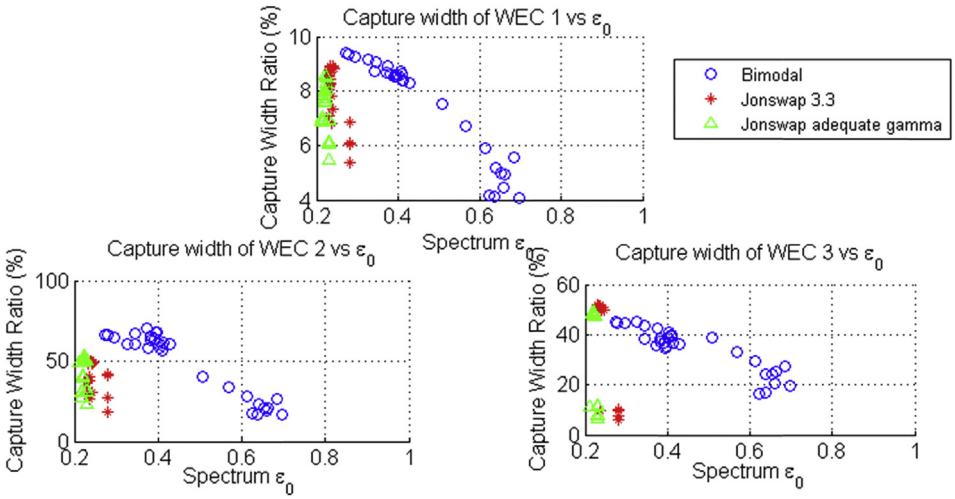

Fig. 15. Capture width ratio versus the broadness parameter for the range of sea states.

From these plots it could be concluded that the influence of bimodal and three modal spectrums on the power production is very high. When assuming an analytical spectrum for a bimodal spectrum the error is large on instantaneous terms and the power production could be over or under estimated by as much as 200%.

Also the capture width ratio is not well estimated assuming one peaked spectrums. A clear tendency is found, that the higher the spectrum broadness the lower the efficiency of the conversion, however this tendency is not captured with one peak spectrums and then it is over or under estimated.

5.2.2. Comparisons on annual energy production

The influence of the shape of the spectrums on the power production on an instantaneous basis has been investigated on the previous section. However, one of the objectives of this paper is estimating the influence of these assumptions on the classical method of power assessment for the annual energy production. The classical method of power assessment consist on the multiplication of the power matrix (kW) by the scatter plot (in percentage) assuming analytical spectrums for the representative sea states on the power matrix.

However, as demonstrated on the previous section only between 30% and 60% of the real states fit with these analytical shapes and then the real power production is not estimated accurately with the classical power production assessment.

Within this research four different approaches are compared. On the one hand, the classical method of multiplying the power matrix by the scatter plot. On the other hand, the computations of

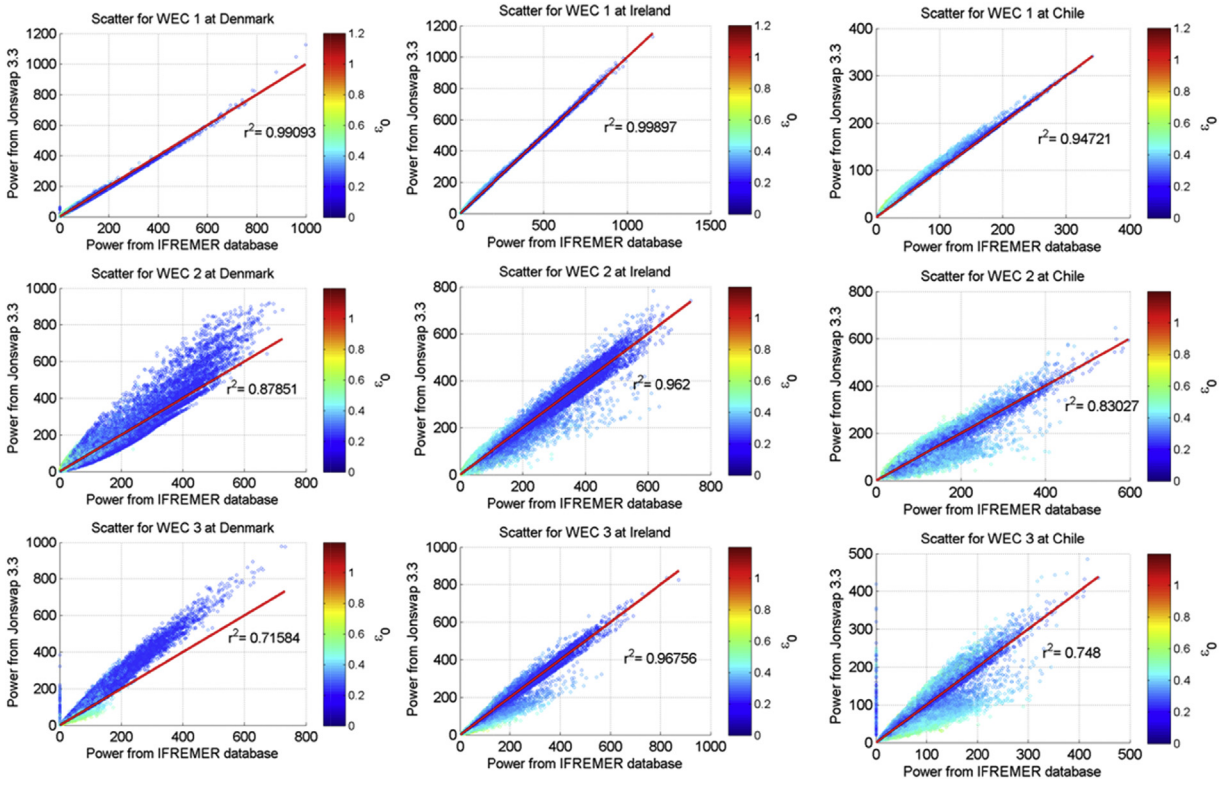

Fig. 16. Comparison scatters for Denmark, Ireland and Chile.

the whole series of sea states (9469 sea states for Bilbao and 58460 for the other sites) with the IFREMER data base (taking into account smoothed bi and tri modal spectrums as well) and the JONSWAPs with $\gamma = 3.3$ and the best γ fit. It should be noticed that the Reference case for the Bilbao locations refers to the AEP calculated with the buoy data (real data) while in the other locations the Reference case refers to the AEP calculated with the IFREMER data due to the absence of buoy data on these locations.

The annual energy production for each alternative is presented in Fig. 17. As expected the highest power production on the three WECs corresponds to Ireland. The lowest power production corresponds to Denmark for WEC1 and WEC2. However for WEC3 the lowest power production corresponds to Chile because it is tuned with a climate that is close to Denmark site.

With respect the differences between the different sets of data they are represented on Table 5. It should be noticed that the percentages are calculated against the most exact case for each location. In Bilbao the percentages are calculated against the buoy data and in the rest locations the percentages are calculated against the IFREMER data. As can be seen the highest differences exist in the Denmark site. This is due to the fact that Denmark is the location with the highest percentage of more than one peak sea states (nearly 60%). Also the differences are higher for the WEC 3 in the Denmark site. This WEC has a peak response near 6 s that is the most probable on this site and also the most probable for the sea states of more than one peak and so these differences are expected. For WEC 3 on Denmark location the JONSWAP spectrum overestimates the mean annual power production by 30%.

For the Denmark location WEC 1 and WEC 2 power production are underestimated with the JONSWAP spectrums. This is due to the fact that on this location the selected sea states are found on the low periods section and this WECs are either tuned for a higher period (WEC2) or do not have a resonance period (WEC1). For the other locations Ireland is the site where the differences are lower. This is due to the fact that the percentage of more than one peak sea states is lower.

Table 6 highlights the differences between the power matrix "classical approach" and the other methods. As it can be seen in all the cases, the highest difference corresponds to Bilbao, where it is compared with real data. The difference goes from −23% for WEC 1 to −32% in WEC 2 and also −44% for the WEC 3. The highest difference correspond to the WEC 3 due to the fact of the peak on its power matrix is on the 6 s area, and the more than one peak spectrums are also located around this area.

For the other locations the differences between power matrix and other methods are found to be in a range of −13% to −7% The differences are also high on the case of Ireland. This is due to the fact that the Ireland scatter plot is very broad, and then in order to get a better definition a smaller cell range would be needed. It should be noticed that these differences of the annual energy production are very high, and then this uncertainty should be taken into account when analysing the techno-economic viability of a device. The power matrix has been demonstrated to be a quick and simple method to obtain the AEP, however, as demonstrated here it is partially inaccurate and then, more accurate methods such as the methodology presented in de Andres et al. (2013) are needed.

With respect the IFREMER case, as it is taken as the most exact for Denmark, Chile and Ireland the comparison is only valid for the Bilbao case. As can be seen, the error percentages goes from 9% to 13 % this is quite low compared to the power matrix errors for the same location (−23% to −44%). It can be concluded that the IFREMER data base can be taken as basis in order to obtain the AEP, as it contents realistic sea states.

For the JONSWAP with $\gamma = 3.3$ and JONSWAP with the best γ fit both generally have a better approximation to the exact AEP than the power matrix method. It can be highlighted that the smaller the

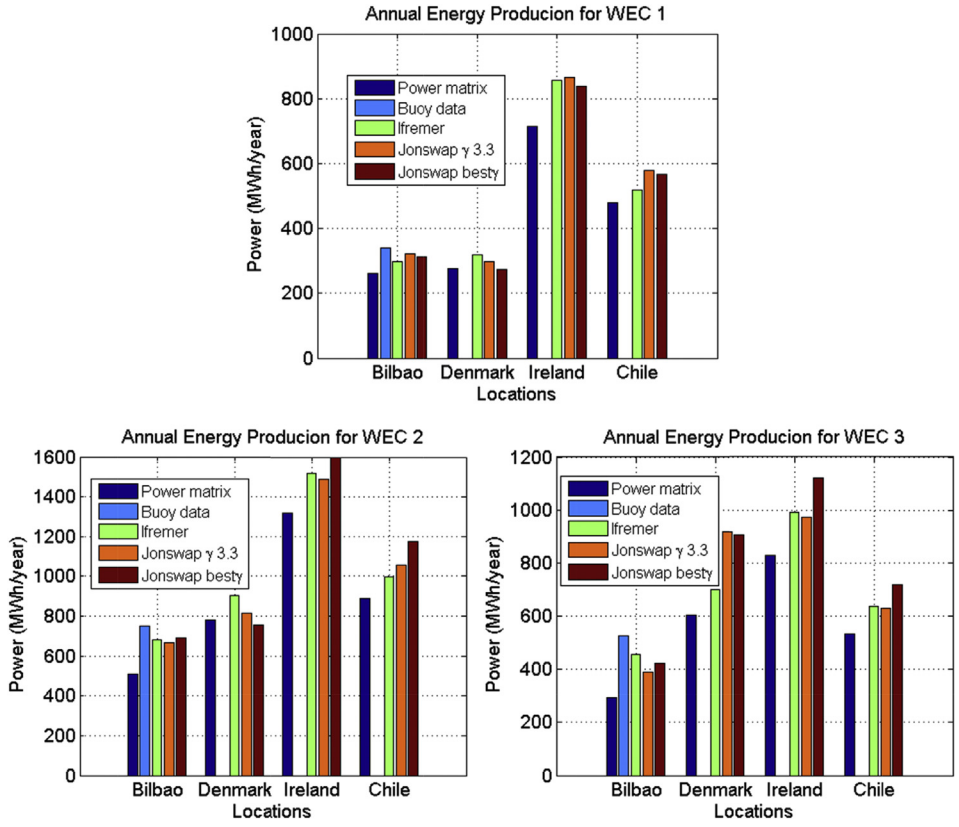

Fig. 17. Annual Energy production for the selected cases.

Table 6
Comparison in % among the different power assessment approaches.

		Power matrix	Buoy data	Ifremer data	JONSWAP $\gamma = 3.3$	JONSWAP best γ fit
WEC 1	Bilbao	−23%	Exact case	−12%	−5%	−8%
	Denmark	−13%	–	Reference case	−6%	−14%
	Ireland	−17%	–	Reference case	1%	−2%
	Chile	−7%	–	Reference case	12%	9%
WEC 2	Bilbao	−32%	Exact case	−9%	−11%	−8%
	Denmark	−13%	–	Reference case	−8%	−16.5%
	Ireland	−13%	–	Reference case	−2%	5%
	Chile	−10%	–	Reference case	−6%	18.2%
WEC 3	Bilbao	−44%	Exact case	−13%	−26%	−20%
	Denmark	−14%	–	Reference case	31%	30%
	Ireland	−16%	–	Reference case	−2%	13%
	Chile	−16%	–	Reference case	−2%	12%

Note: For Bilbao the comparison is with Buoy data while for other locations the comparison is with IFREMER data.

power matrix cell size the more proximate to the JONSWAP with $\gamma = 3.3$ results. Then, the difference on the error with these two methods rely on the cell size of the power matrix. The highest overestimation with these 2 approaches correspond to Denmark with the WEC 3 case. As explained before this WEC has a peak on the 6 s area and then as this is the most probable period in Denmark the overestimation is very important. For the other cases the underestimation is lower for the WEC 1 case as it works as a follower and its power matrix is smoother.

5.2.3. Resource and capture width comparisons

When comparing different types of devices one important parameter is the capture width ratio, that measures the efficiency of the conversion with respect the incident resource (see Equation (1)). In order to assess this parameter an assessment of the available resource in the selected locations is useful.

Based on the different sources of data used in the previous sections the average resource is estimated. This resource is calculated frequency component by component of the wave spectrum and for each spectrum. The average resource is shown in Fig. 18. For Denmark, Ireland and Chile the wave resource is heavily overestimated by the JONSWAP spectrums. On average, the wave energy resource is overestimated on a 30% using a JONSWAP with $\gamma = 3.3$. Also as can be seen, the other JONSWAP approximation (with an adequate γ fit) has a lower underestimation of the resource (around 20%). For the Bilbao location (that is the only one with buoy data) the resource is underestimated compared to the buoy by the IFREMER and the JONSWAP data. However, if the attention is fixed on the IFREMER and the JONSWAP data they again overestimate the resource. If the two JONSWAP approaches are compared it can be seen how the approach with $\gamma = 3.3$ is the one that overestimates with a higher percentage. The JONSWAP with the γ fit overestimates the resource with a lower percentage. This means that if the γ is fit to the different shapes of the spectrum (differentiating between wind sea and swell) the overestimation is lower.

In Fig. 19 the Capture Width Ratio is represented for all the data sources. It should be pointed out that on the capture width estimation both the power production uncertainties and the resource are mixed and then the comparison between the different sources is expected to be worse.

On average terms the WEC 1 has a CWR around 7%. It is quite low due to the fact that is a follower and as it is not designed to resonate their performance is low. For the second converter their average CWR goes to 60%, that is quite high due to its resonance. However it is suspected that this CWR is overestimated due to the fact that the model used for this computation is linear. In reality, this type converter would have a lower performance. For the WEC 3, its average CWR goes to 25%, that is standard on these type of devices.

With respect the comparisons between the different CWR for the different type of data it can be seen how the JONSWAP spectrums underestimate heavily the average CWR. This fact is coherent as in general the power production is underestimated by the JONSWAP and the resource is heavily overestimated. Then, the CWR is heavily underestimated by the JONSWAP series. The highest differences correspond to Denmark, that as specified before is the location with the highest occurrence of bi and tri-peaked sea spectrums.

6. Conclusions

This paper presents an extension of the work initiated by Ref. [1] regarding a time-efficient methodology to estimate the long-term power performance of a device. This methodology uses a sea state selection technique in order to select the most distinct and representative sea states from a long-term spectrum data series. These selected sea states are the input for a numerical model (frequency domain in this paper) and the power production for the cases is assessed. Afterwards a non-linear interpolation technique (RBF functions) is used in order to reconstruct the whole power production series along the met-ocean data series.

The influence of several factors on the aforementioned methodology has been investigated. In this work three types of WECs, a one body heaving converter (a wave follower, “non-resonant”, low pass response), a two body heaving converter (“resonant”, band

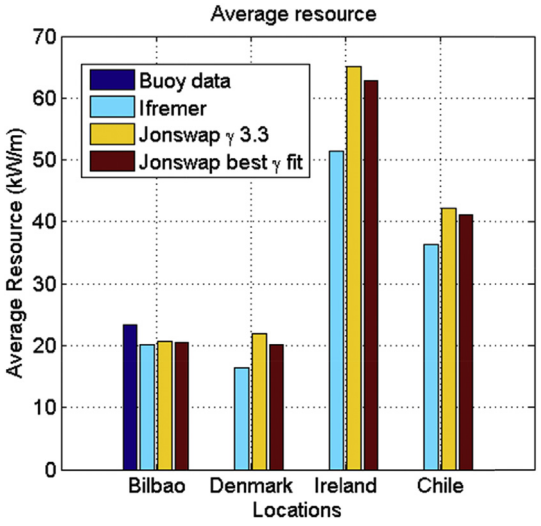

Fig. 18. Resource estimation for the different locations.

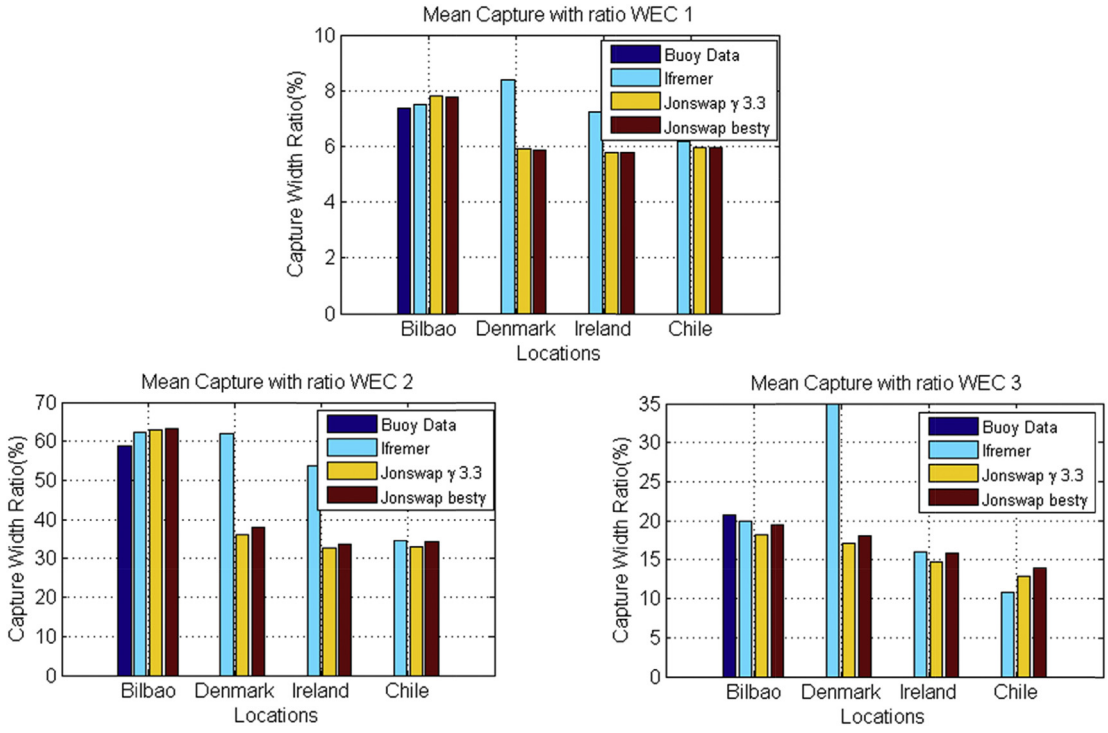

Fig. 19. Capture width ratio for the different variants.

limited response) and a deep water flap has been investigated ("non-resonant", band limited response). Regarding the locations 4 different locations with different scatter plot and sea-states distribution characteristics were assessed (Bilbao- North of Spain, West of Denmark, West of Ireland and Chile). A set of simulations was run in order to investigate the influence of these factors on the methodology.

The methodology was found to work well with the different types of WECs, locations and types of data. It was concluded to work more accurately with converter that is not band limited in frequency response, as its response is more smooth and then with a lower number of cases a very good precision is achieved. With respect the data types a selection based on H_{m0},T_p and ε_0 was found to be very efficient for the real spectrums with more than 1 peak. However for the JONSWAP cases a selection based on two parameters H_{m0} and T_p was found to be enough because the ε_0 masked the variability of the data (as all of them were 1 peaked spectrums).

The influence of the real spectrums in contrast to the analytical spectrums (JONSWAP), was investigated. On sea-state by sea-state terms the differences were very high (±200%).

The inaccuracy of the classical method of computing the AEP was investigated in this paper. These approach was compared with the others set of data. The power matrix method was found to under/overestimate the AEP on all the locations from −45% to −7%.

Also the computation of the whole sea states data series with JONSWAP spectrums made to an underestimation of −20% to −5% in the AEP. The critical location for this comparison was found to be Denmark, as the percentage of one peaked sea states is just 40%. The classical power matrix method was found to be very inaccurate in this type of locations.

Also the resource was investigated on this research. The assumption of JONSWAP spectrums for an specific H_{m0},T_p set lead to an overestimation of the resource of a 30% in all the locations. Also the CWR estimation based on JONSWAP spectra was found to be very inaccurate due to the errors in both the resource and the power production. To sum up, the classical method of power production assessment was found to be very inaccurate in areas with high percentage of combined wind sea-swell sea states. Generally, the influence of real spectrums with respect analytical ones was found to be very important and then for a power production assessment series with real spectrum shapes is recommended.

Acknowledgements

The authors gratefully acknowledge the financial support from the University of Cantabria to the PhD student Adrian de Andres through its PhD scholarships students program. The authors also acknowledge Antonio Tomas, from IH Cantabria who kindly provided the buoy data and the IFREMER data for this study and Paula Camus that helped Adrian with the RBF interpolation methodology. The authors are grateful for Spanish Ministry of Economy and Competitiviness and in particular to the State Secretariat for Research, Development and Innovation funding for VAPEO – Ocean Climate Variability influence over Wave Energy Converters Power Production project (ENE2013-48716-R), within the National Programme for Research Aimed at the Challenges of Society, modality 1, Research Challenge: Research, Development and Innovation.

References

[1] Andres AD, Guanche R, del Jesus F, Vidal C, Losada IJ. Time domain model of a teo body heave converter: model and applications. Ocean Eng 2013 November;72:116–23.
[2] Guanche R, de Andres A, Simal PD, Vidal C, Losada IJ. Uncertainty analysis of wave energy farms financial indicators. Renew Energy 2014 August;68:570–80.
[3] Snarey M, Terrett NK, Willett P, Wilton DJ. Comparison of algorithms for dissimilarity-based compound selection. J Mol Graph Model 1997;15:372–85.
[4] Franke R. Scattered data interpolation: tests of some method. Math Comput 1982;38:181–200.
[5] Camus P, Mendez F, Medina R, Cofiño A. Analysis of clustering and selection algorithms for the study of multivariate wave climate. Coast Eng 2011 June;58:453–62.

[6] Babarit A, Hals J, Muliawan MJ, Kurniawan A, Moan T, Krokstad J. Numerical benchmarking study of a selection of wave energy converters. Renew Energy 2011;41.
[7] Kerbiriou M, Prevosto M, Maisondieu C, Babarit A, Clement A. Influence of an improved sea-state description on a wave energy converter production. In: Proceedings of the 26th International Conference on Offshore Mechanics and Artic Engineering; 2007 [San Diego, California, USA].
[8] Kerbiriou M, Prevosto M, Maisondieu C, Clement A, Babarit A. Influence of sea-states description on wave energy production. In: Proceedings of the European Wave and Tidal Energy Conference; 2007 [Porto].
[9] Saulnier J, Clement A, Falcao A, Pontes T, Prevosto M, Ricci P. Wave groupiness and spectral bandwidth as relevant parameters for the performance assessment of wave energy converters. Ocean Eng 2011 January;38(1).
[10] Saulnier J, Prevosto M, Maisondieu C. Refinements of sea state statistics for marine renewables: a case study from simultaneous buoy measurements in Portugal. Renew Energy 2011;36(11).
[11] Falnes J. Ocean waves and oscillating systems. Cambridge University Press; 2002.
[12] Goda. Random seas and design of maritime structures, vol. 133; 2000. p. 367. p. equation 10.
[13] Seactricity. [Online]. Available from: http://www.seatricity.net/.
[14] Seabased. [Online]. Available from: http://www.seabased.com/en/.
[15] OPT Power buoy. [Online]. Available from: http://www.oceanpowertechnologies.com/.
[16] Wavebob. [Online]. Available from: http://en.wikipedia.org/wiki/Wavebob.
[17] Fronde WEC. [Online]. Available from: http://www.see.ed.ac.uk/~eeto/Modules%20-%20do%20not%20use/45–07/Handouts/wave/The%20Frond%20Wave%20Energy%20Generator.pdf.
[18] Salter S. The swinging mace. In: Proceedings of the workshop wave energy R&D; 1992. p. 197–206.
[19] Wang DW, Hwang PA. An operational method for separating wind sea and swell from ocean wave Spectra. J Atmos Ocean Technol 2001;18.
[20] Rascle N, Ardhuin F, Queffeulou P, Croizé-Fillon D. A global wave parameter database for geophysical applications. Part 1: wave–current–turbulence interaction parameters for the open ocean based on traditional parameterizations. Ocean Model 2008;25:154–71.
[21] Rascle N, Ardhuin F. A global wave parameter database for geophysical applications. Part 2: model. Ocean Model 2013 October;70:174–88.
[22] Hanson J, Philips O. Automated analysis of ocean surface directional wave spectra. J Atmos Ocean Technol 2001;18:277–93.
[23] Tracy B, Devaliere E, Hanson J, Nicolini T, Tolman H. Wind sea and swell delineation for numerical wave modeling. In: Proc. 10th int. workshop on wave hindcasting and forecasting; 2007.